Angewandte Zuschriften

Photocatalysis

DOI: 10.1002/ange.201303693

Core/Shell Photocatalyst with Spatially Separated Co-Catalysts for Efficient Reduction and Oxidation of Water**

*Daoai Wang, Takashi Hisatomi, Tsuyoshi Takata, Chengsi Pan, Masao Katayama, Jun Kubota, and Kazunari Domen**

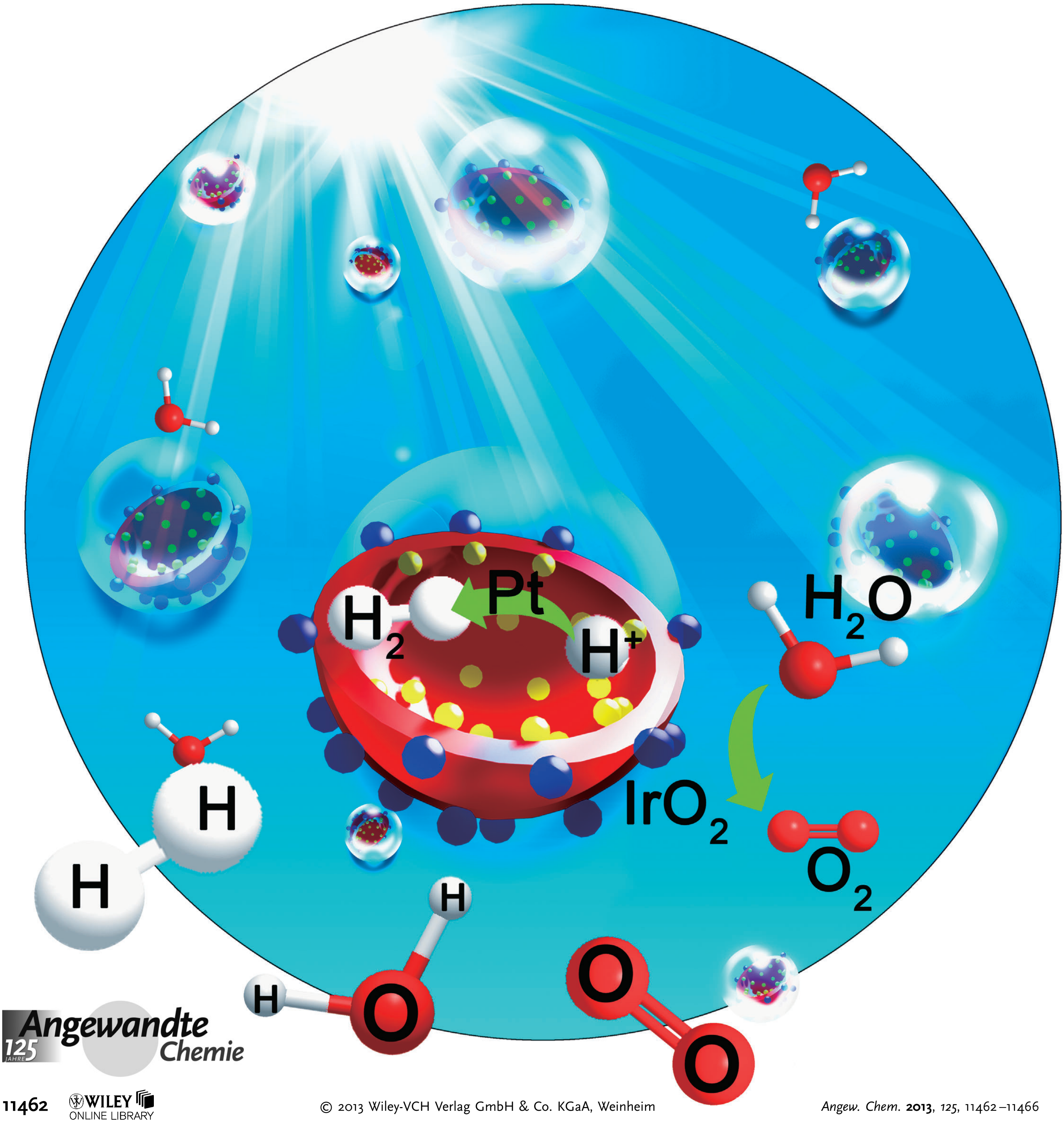

In recent years the photocatalytic water splitting used for the generation of clean and renewable H_2 energy has attracted more and more attention because of energy and environmental issues. To date, many metal-oxide photocatalysts have enabled great advances in the decomposition of water into H_2 and O_2 under ultraviolet irradiation.[1–3] Some visible-light-driven photocatalysts have also been studied extensively, including series of nitrides, oxynitrides, oxysulfides, and their composites, although the quantum efficiency is still too low for commercial use.[4–10] Among these, tantalum nitride (Ta_3N_5) with a band gap of 2.1 eV (absorption edge at 610 nm) is considered to be one of the most promising candidates for water splitting under visible light. Despite intense efforts in previous works,[6,11–13] research on Ta_3N_5 photocatalyst for solar water splitting has progressed at a slow pace with very low H_2 evolution activity, and the overall water splitting has not yet been achieved. The recombination of photoexcited electrons and holes in the bulk material is one of the most detrimental factors negatively impacting the photocatalytic activity. Another possible reason is the in situ reverse reaction of the as-formed H_2 and O_2 to form H_2O again on the surface of the photocatalyst.

Innovation in the structure and morphology of photocatalytic materials is one key to enhancing the charge separation and transfer efficiency as well as increasing the density of reaction sites. Earlier studies have revealed that ordered one-dimensional structures and nanocrystalline monolayer structures can accelerate the separation and transfer of photon-induced electrons and holes as well as increase the efficiency of the process.[14–16] In addition, suitable cocatalysts can improve the reduction and oxidation activities of water by an order of magnitude or even more. So far, various noble metals, such as Pt and Pd, have been reported to act as effective cocatalysts for the reduction of water to form H_2, whereas some metal oxides, such as RuO_2, IrO_2, and CoO_x, have performed better as cocatalysts for the oxidation of water to form O_2.[17] Therefore, loading both H_2 and O_2 evolution cocatalysts onto the same photocatalyst should improve the water splitting activity further, owing to the accumulative catalytic effect and rectified charge transport. Unfortunately, till now, few successful and reliable models of this have been reported.[18–20] The cocatalysts were usually deposited on the surface randomly. The full advantage of loading both reduction and oxidation sites, that is, rectified charge separation, could not be demonstrated.

Herein, we present a novel and simple method for preparing core/shell photocatalysts modified with spatially separated cocatalysts to enhance their water-splitting activity. Taking the Ta_3N_5 photocatalyst as an example, we show a proof-of-concept using a SiO_2/Ta_3N_5 core/shell photocatalyst loaded with Pt nanoparticles (NPs) on the inner Ta_3N_5 shell surface as an electron collector and IrO_2 or CoO_x on the outer shell surfaces as a hole collector, respectively (see Figure 1 a). This core/shell structure with separated cocatalysts has at least two advantages: 1) the core/shell structure with controllable architecture has a larger surface area and more active sites than the bulk material, which is advantageous for photocatalytic reactions, and 2) having separated cocatalysts facilitates the separation and migration of photoexcited electrons toward the inner and outer surfaces, thereby decreasing recombination as well as the reverse reaction.

Owing to its simplicity and controllability of particle size and shape, transparent spherical silica was employed as a hard template in this study. The amorphous tantala derived from the hydrolysis of $Ta(OEt)_5$ was first coated on the surfaces of Pt NP-loaded silica spheres to form the $Ta_2O_5/Pt/SiO_2$ core/shell structure. After nitridation in ammonia gas, the $Ta_3N_5/Pt/SiO_2$ (TPS) core/shell structure was obtained. Subsequently, IrO_2 or CoO_x NPs were deposited on the outer surface of TPS as a second cocatalyst to form the final photocatalyst (see Figure 1 a and Scheme S1 in the Supporting Information). The SiO_2 cores can also be selectively dissolved in a hot NaOH solution to fabricate Ta_3N_5/Pt (TP) hollow sphere photocatalysts. More details on the synthesis of

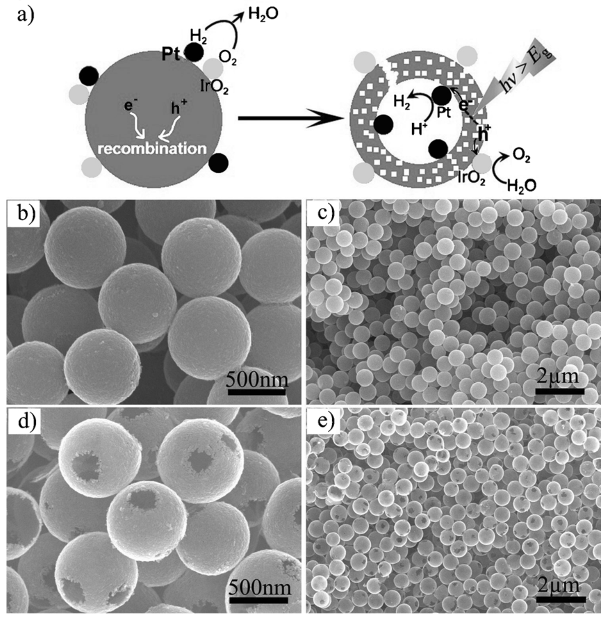

Figure 1. a) Design principle, which involves the use of two separated cocatalysts on the core/shell Ta_3N_5 photocatalyst as effective charge collectors for water splitting. b,c) SEM images of the $Ta_3N_5/Pt/SiO_2$ photocatalyst with 1 wt% Pt NPs loaded between the Ta_3N_5 shell and SiO_2 core. d,e) SEM images of Ta_3N_5/Pt hollow spheres from $Ta_3N_5/Pt/SiO_2$ core/shells after removal of the SiO_2 core in a hot NaOH solution.

---

[*] Dr. D. Wang, Dr. T. Hisatomi, Dr. T. Takata, Dr. C. Pan,
Prof. M. Katayama, Prof. J. Kubota, Prof. K. Domen
Department of Chemical System Engineering
The University of Tokyo
7-3-1 Hongo, Bunkyo-ku, Tokyo 113-8656 (Japan)
E-mail: domen@chemsys.t.u-tokyo.ac.jp

[**] This work was supported in part by a Grant-in-Aid for specially promoted research of the Japan Society for the Promotion of Science (JSPS) (grant number 23000009) and the Advanced Low Carbon Technology Research and Development Program (ALCA) of the Japan Science and Technology Agency (JST). This work also contributes to the international exchange program of the A3 Foresight Program of JSPS. One of the authors (D. Wang) appreciates the support from JSPS.

Supporting information for this article is available on the WWW under http://dx.doi.org/10.1002/anie.201303693.

core/shell Ta_3N_5/SiO_2 (TS) and modification treatments are available in the Supporting Information and Figure S1.

Figure 1 b–c shows typical scanning electron microscopy (SEM) images of as-prepared monodisperse TPS core/shell photocatalysts. The key to prepare core/shell photocatalysts is that the hydrolysis rate of $Ta(OEt)_5$ can be controlled by adding a small amount of glacial acetic acid.[21] Upon nitridation, the smooth Ta_2O_5 shell transforms into a nanoporous Ta_3N_5 shell with wormhole-like structures (Figure S1). This porosity not only increases the surface area but also makes the reaction solution accessible to the active sites where Pt NPs work as a H_2 evolution promoter. After removing the SiO_2 core, monodisperse Ta_3N_5 hollow spheres with a thickness of about 40 nm can be obtained, as shown in Figure 1 d–e. The successful formation of hollow spheres confirms the high uniformity of the tantala coating on the SiO_2 templates. Interestingly, as shown in Figure 1 d, there were some large holes (200–300 nm) on the surface of the Ta_3N_5 hollow spheres, originating from a thinner part of the Ta_3N_5 shell. This is actually beneficial for enhancing the exchange rate of the solution between the inside and outside of the hollow spheres. More detailed characterization of the core/shell photocatalysts with controllable shell thicknesses, lower absorption background indicative of fewer defects, and large surface areas are shown in Figure S2.

To form a core/shell photocatalyst with separated cocatalysts, a blue IrO_2 colloid (0.005–2 wt %) was loaded on the TPS photocatalysts by stirring them for 12 h at room temperature. A cobalt oxide cocatalyst was also deposited onto the TPS samples by an impregnation method followed by heat-treatment in NH_3. These samples were evaluated by X-ray photoelectron spectroscopy, as shown in Figure S3 in the Supporting Information. The peak positions were in good agreement with those for Co^{2+} and Co^{3+} ions reported in the literature.[22,23] This cocatalyst is referred to as CoO_x for simplicity. To confirm the core/shell Ta_3N_5 photocatalyst with spatially separated cocatalysts, the morphologies of the above samples were detected by transmission electron microscopy (TEM) and SEM. Figure 2 a shows the low-magnification image of a cracked Ta_3N_5 hollow sphere with separated cocatalysts of CoO_x NPs on the outer shell surface and Pt NPs on the inner shell surfaces. We observed in the high-magnification images of the cracked Ta_3N_5 hollow sphere that Pt NPs about 3–5 nm in diameter were loaded on the inner shell surface (Figure 2 c) whereas CoO_x NPs about 20 nm in diameter were loaded on the outer shell surface of the Ta_3N_5 hollow sphere (Figure 2 b). The CoO_x NPs on the outer surface of Ta_3N_5 spheres were further confirmed by the SEM shown in Figure 2 d. The high-resolution TEM (HRTEM) image in Figure 2 e reveals that the core/shell Ta_3N_5 photocatalyst and the loaded Pt cocatalyst were crystalline. The marked lattice spacings of approximately 3.62 and 2.27 Å agreed well with the (110) and (100) planes of Ta_3N_5 and Pt, respectively. More HRTEM images are presented in Figure S4.

To investigate the effect of the structure of the photocatalysts on their activity, the half reactions for H_2 and O_2 evolution were tested under visible light. The representative results were tabulated in Tables S1 and S2, respectively. Figure 3 a shows the time courses of H_2 evolution for the TP hollow sphere, TPS core/shell, and bulk Ta_3N_5 photocatalysts. The average H_2 evolution rates in the first 5 h were calculated to be approximately 6.6, 3.1, and 0.5 μmol h^{-1}, respectively. The core/shell or hollow sphere photocatalysts showed a significantly enhanced performance in comparison with bulk Ta_3N_5 photocatalysts owing to the large surface area and the low density of reduced Ta species. In the core/shell TPS, Pt still acts as a H_2 evolution cocatalyst despite being loaded between the SiO_2 core and the Ta_3N_5 shell. This means that the solution was able to infiltrate the Ta_3N_5 shell through the nanopores and wormhole-like structures. Note that the activity was further improved by removing the SiO_2 core and thus exposing more Pt NPs on the inner surface of the Ta_3N_5 shell to the reaction solutions. The hollow sphere Ta_3N_5 photocatalysts have good stability during the H_2 evolution process, as shown in Figure S5.

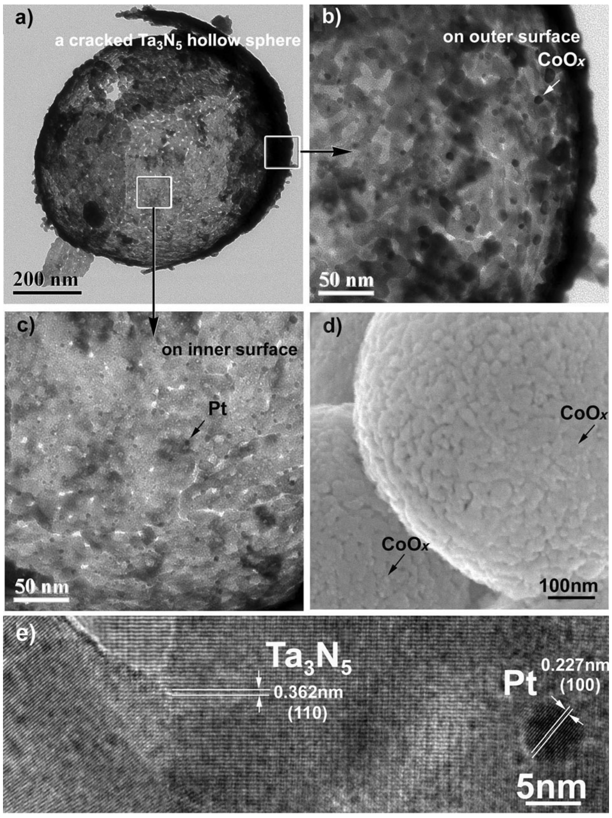

Figure 2. a–c) TEM images of a cracked Ta_3N_5 hollow sphere with spatially-separated CoO_x on the outer shell surface (b) and Pt NP cocatalysts on the inner Ta_3N_5 shell surface (c). d) SEM images of core/shell Ta_3N_5 photocatalyst with 2 wt % CoO_x cocatalyst loaded on the outer shell surface. e) HRTEM of Ta_3N_5 hollow sphere loading with Pt NPs.

Figure 3 b shows the time courses of H_2 evolution on core/shell Ta_3N_5 photocatalysts loaded with separated and mixed IrO_2 and Pt cocatalysts. The average H_2 evolution rate of TPS was increased by approximately 50 % upon loading 0.025 wt % IrO_2 cocatalyst on the outer surface. However, a further increase in the IrO_2 loading amount to 0.5 wt % decreased the H_2 evolution rate, as shown in Figure 3 b and Figure S6a. The loading location of the cocatalysts also played

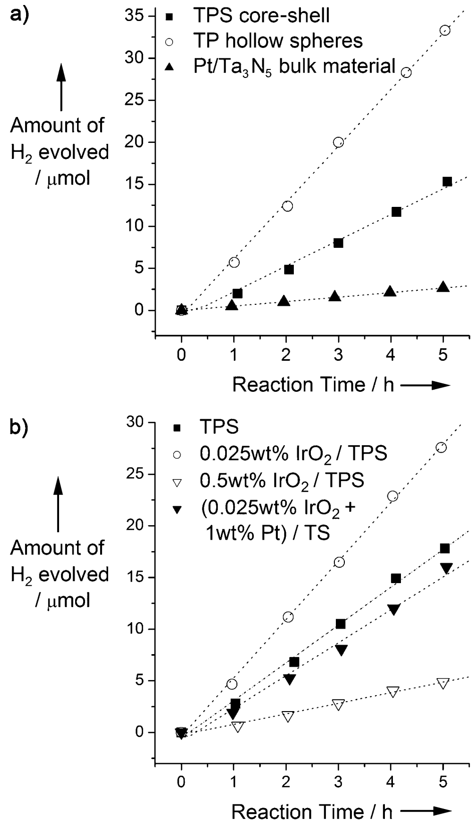

Figure 3. a) Time courses of H_2 evolution on TPS core/shells, TP hollow spheres, and bulk Ta_3N_5 photocatalysts. b) H_2 evolution activities on core/shell Ta_3N_5 photocatalysts with separated and mixed Pt and IrO_2 cocatalysts. Reaction conditions: 0.032 g Ta_3N_5 catalyst; 20 mL methanol and 80 mL H_2O; 300 W Xe lamp with an L42 cutoff filter, top irradiation.

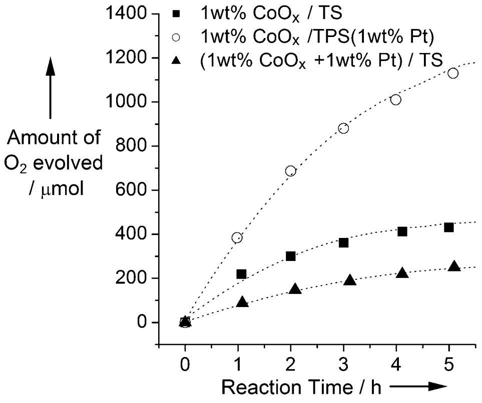

Figure 4. Time courses of O_2 evolution on core/shell Ta_3N_5 photocatalysts with and without spatially separated cocatalysts, using CoO_x as an O_2 evolution promoter. Reaction conditions: 0.032 g Ta_3N_5 photocatalyst; 200 mL 0.02 M $AgNO_3$ (aq.) containing 0.2 g of La_2O_3 as a buffer; 300 W Xe lamp with an L42 cutoff filter, top irradiation.

a crucial role in H_2 evolution. For comparison, both 1 wt% Pt and 0.025 wt% IrO_2 were loaded on the outer surface of the TS core/shell photocatalyst. As shown in Figure 3b, the activity of the resulting sample decreased even at the optimal loading amount of IrO_2. This suggests that the photocatalytic activity of Ta_3N_5 can be further improved by introducing the core/shell structure with separated cocatalysts. The above concept and new model of a core/shell photocatalyst with separated cocatalysts on the inner and outer surface are thus demonstrated to be effective.

Physically separated loading of reduction and oxidation cocatalysts on the core/shell photocatalysts also improved the O_2 evolution performance. Figure 4 shows the time courses of O_2 evolution over core/shell photocatalysts with different cocatalyst loading types, including 1 wt% CoO_x-loaded TS, 1 wt% CoO_x-loaded TPS, and TS photocatalysts with mixed loading (1 wt% CoO_x + 1 wt% Pt) on the outer surfaces. The O_2 evolution rates in the first hour were calculated to be approximately 202, 392, and 88 µmol h^{-1}, respectively. These results highlight the positive effect that the separated loadings of CoO_x and Pt cocatalysts have on the separation of photoexcited electrons and holes during the O_2 evolution reaction. However, the quantum efficiency was still low. The importance of the core/shell photocatalyst with separated cocatalysts was also confirmed when IrO_2 was used as an additional O_2 evolution promoter resulting in doubled photocatalytic activity as shown in Figure S6b. The loading amount of Pt and CoO_x also played an important role in the O_2 evolution activity, as shown in Figure S6c. The core/shell Ta_3N_5 photocatalyst with 1 wt% Pt on the inner shell surface and 1 wt% CoO_x on the outer shell surface has the best water oxidation activity in the presence of Ag^+.

To clarify the effect of the Pt cocatalyst for the oxidation of water, the O_2 evolution experiments using Ta_3N_5/Pt hollow spheres and unplatinized Ta_3N_5 hollow spheres were performed, and the morphology of the sample after the reaction were characterized by SEM (Figure S7). Ag NPs were mainly deposited on the inner surface of Ta_3N_5 hollow spheres, where the Pt NPs were loaded. However, without loading the Pt catalyst, only a small amount of Ag particles with smaller size formed as shown in Figure S7c and S7d. Clearly, it is easier to reduce Ag NPs on a Pt-modified shell surface than on a bare Ta_3N_5 surface, which indicates that the Pt cocatalyst serves as an electron collector, promoting the oxidation of water by enhancing the reduction of Ag^+ ions.

Despite the significant improvement in the photocatalytic activity for sacrificial H_2 and O_2 evolution, the core/shell Ta_3N_5 modified with spatially separated cocatalysts did not show activity for overall water splitting in the absence of sacrificial reagents. Charge separation based on the spatially separated loading of cocatalysts was not sufficient likely because of Schottky barriers at the interfaces of Ta_3N_5 and the cocatalysts. In our previous study, it was found that a Schottky barrier at the interface of an n-type GaN single crystal and Pt particles prevented injection of photoexcited electrons from GaN to Pt, whereas a part of the photoexcited holes could be injected into Pt, when the potential of the n-type GaN was more positive than the flat band potential.[24] In the present case, the absence of methanol would limit the shift in the quasi-Fermi level of electrons under photoexcitation. As a result, photoexcited electrons could not overcome a Schottky barrier, recombining with holes. A similar concept should hold regarding the behaviors of photoexcited holes in the presence and absence of sacrificial electron acceptors. Accordingly, we consider that selective electron and hole injection to H_2 and O_2 evolution cocatalysts should necessitate ohmic contacts at the respective interfaces in addition to physical separation of the cocatalysts. The step-by-step process presented in this work will offer a shortcut to such elaborate systems. Further investigation on core/shell photocatalysts and physically separated cocatalysts is in progress to achieve overall water splitting. Note that the present study also provides a facile and universal route to prepare a series of core–shell and hollow sphere materials, such as TiO_2, Nb_2O_5, TaON, $BaTaO_2N$, and so on, with tunable morphology, component, and separated cocatalysts by simple sol–gel and template approaches (Figure S8). It is also expected that the present method can open up a new area in nanotechnology research to prepare various heterojunction materials by this method, which have wide applications in photocatalysts, sensors, solar cells, electronic filters, and drug delivery carriers.

In summary, we have demonstrated a simple method to prepare the core/shell photocatalysts with spatially separated cocatalysts to improve the photocatalytic activity. The resulting core/shell Ta_3N_5 photocatalyst, the inner and outer surfaces of which were modified with Pt and IrO_2 NPs, respectively, showed significantly enhanced water reduction and oxidation performance under visible light irradiation. The high activity was attributed to the core/shell structure and separated cocatalysts that assisted separation and collection of the electrons and holes at the respective cocatalysts, owing to active rectification of electron and hole transport. The ease and reproducibility of this synthetic approach is expected to extend to the production of other heterojunction photocatalysts with controllable morphology and components having potential applications in areas of energy conversion and environmental cleanup.

Received: April 30, 2013
Revised: July 28, 2013

Keywords: core/shell materials · electrochemistry · green chemistry · photocatalysis · water splitting

---

[1] A. Fujishima, K. Honda, *Nature* **1972**, *238*, 37–38.
[2] K. Domen, A. Kudo, T. Onishi, N. Kosugi, H. Kuroda, *J. Phys. Chem.* **1986**, *90*, 292–295.
[3] A. Kudo, H. Kato, *Chem. Phys. Lett.* **2000**, *331*, 373–377.
[4] K. Maeda, T. Takata, M. Hara, N. Saito, Y. Inoue, H. Kobayashi, K. Domen, *J. Am. Chem. Soc.* **2005**, *127*, 8286–8287.
[5] K. Maeda, K. Teramura, D. Lu, T. Takata, N. Saito, Y. Inoue, K. Domen, *Nature* **2006**, *440*, 295.
[6] M. Hara, G. Hitoki, T. Takata, J. N. Kondo, H. Kobayashi, K. Domen, *Catal. Today* **2003**, *78*, 555–560.
[7] X. Wang, K. Maeda, A. Thomas, K. Takanabe, G. Xin, J. M. Carlsson, K. Domen, M. Antonietti, *Nat. Mater.* **2009**, *8*, 76–80.
[8] F. Zhang, K. Maeda, T. Takata, K. Domen, *Chem. Commun.* **2010**, *46*, 7313–7315.
[9] M. Higashi, K. Domen, R. Abe, *Energy Environ. Sci.* **2011**, *4*, 4138–4147.
[10] R. Abe, M. Higashi, K. Domen, *J. Am. Chem. Soc.* **2010**, *132*, 11828–11829.
[11] T. Hisatomi, M. Otani, K. Nakajima, K. Teramura, Y. Kako, D. Lu, T. Takata, J. N. Kondo, K. Domen, *Chem. Mater.* **2010**, *22*, 3854–3861.
[12] T. Takata, D. Lu, K. Domen, *Cryst. Growth Des.* **2011**, *11*, 33–38.
[13] M. Tabata, K. Maeda, M. Higashi, D. Lu, T. Takata, R. Abe, K. Domen, *Langmuir* **2010**, *26*, 9161–9165.
[14] Q. Wang, K. Zhu, N. R. Neale, A. J. Frank, *Nano Lett.* **2009**, *9*, 806.
[15] R. Yan, D. Gargas, P. Yang, *Nat. Photonics* **2009**, *3*, 569–576.
[16] Y. Lin, S. Zhou, S. W. Sheehan, D. Wang, *J. Am. Chem. Soc.* **2011**, *133*, 2398–2401.
[17] K. Maeda, K. Domen, *J. Phys. Chem. Lett.* **2010**, *1*, 2655–2661.
[18] J. Yang, H. Yan, X. Wang, F. Wen, Z. Wang, D. Fan, J. Shi, C. Li, *J. Catal.* **2012**, *290*, 151–157.
[19] K. Maeda, A. Xiong, T. Yoshinaga, T. Ikeda, N. Sakamoto, T. Hisatomi, M. Takashima, D. Lu, M. Kanehara, T. Setoyama, T. Teranishi, K. Domen, *Angew. Chem.* **2010**, *122*, 4190–4193; *Angew. Chem. Int. Ed.* **2010**, *49*, 4096–4099.
[20] S. Ma, K. Maeda, R. Abe, K. Domen, *Energy Environ. Sci.* **2012**, *5*, 8390–8397.
[21] M. Agrawal, A. Pich, S. Gupta, N. E. Zafeiropoulos, P. Simon, M. Stamm, *Langmuir* **2008**, *24*, 1013–1018.
[22] F. Zhang, A. Yamakata, K. Maeda, Y. Moriya, T. Takata, J. Kubota, K. Teshima, S. Oishi, K. Domen, *J. Am. Chem. Soc.* **2012**, *134*, 8348–8351.
[23] J. Jansson, A. E. C. Palmqvist, E. Fridell, M. Skoglundh, L. Osterlund, P. Thormahlen, V. Langer, *J. Catal.* **2002**, *211*, 387–397.
[24] M. Yoshida, A. Yamakata, K. Takanabe, J. Kubota, M. Osawa, K. Domen, *J. Am. Chem. Soc.* **2009**, *131*, 13218–13219.